

Denoising and Completion of 3D Data via Multidimensional dictionary learning

Zemin Zhang, Shuchin Aeron
Department of EECS, Tufts University
Medford, MA 02155, USA

zemin.zhang@tufts.edu, shuchin@ece.tufts.edu

Abstract

In this paper a new dictionary learning algorithm for multidimensional data is proposed. Unlike most conventional dictionary learning methods which are derived for dealing with vectors or matrices, our algorithm, named K-TSVD, learns a multidimensional dictionary directly via a novel algebraic approach for tensor factorization as proposed in [3, 12, 13]. Using this approach one can define a tensor-SVD and we propose to extend K-SVD algorithm used for 1-D data to a K-TSVD algorithm for handling 2-D and 3-D data. Our algorithm, based on the idea of sparse coding (using group-sparsity over multidimensional coefficient vectors), alternates between estimating a compact representation and dictionary learning. We analyze our K-TSVD algorithm and demonstrate its result on video completion and multispectral image denoising.

1. Introduction

Sparsity driven signal processing has been widely used in many areas across computer vision and image analysis, such as image restoration and classification [1, 16, 21]. The main principle driving the gains is the idea of sparse coding, i.e. the underlying signal is compactly represented by a few large coefficients in the overcomplete dictionary, while the noise and the sampling process are incoherent. Since the performance heavily relies on the chosen dictionary, a lot of dictionary learning algorithms are developed to obtain dictionaries that are more adapted to the signal than the predefined ones, such as wavelet and DCT. In [1], Aharon *et al.* proposed an algorithm called K-SVD, which efficiently learns an overcomplete dictionary from a set of training signals. The method of optimal directions (MOD) [7] shares the same effective sparse coding principle for dictionary learning as K-SVD. Discriminative K-SVD algorithm (DKSVD) proposed in [22] improved the K-SVD method by unifying the dictionary and classifier learning processes. [18] efficiently accelerated the K-SVD algorithm and reduced its memory consumption using a batch orthogonal

matching pursuit method.

When the signal is not limited to two dimensional signals, traditional methods generally embed the high dimensional data into a vector space by vectorizing the data points; therefore the conventional matrix based approaches can still be used. This kind of vectorization, however, will lead to a poor sparse representation since it breaks the original multidimensional structure of the signal and reduce the reliability of post processing. To this end, some dictionary learning techniques have been explored based on different tensor decompositions such as CP decomposition [5, 11], Tucker Decomposition [9, 15, 24] and tensor-SVD [19]. In [5], the authors developed an algorithm called K-CPD which learns high order dictionaries based on the CP decomposition. [24] proposed a tensor dictionary learning algorithm based on the Tucker model with sparsity constraints over its core tensor, and applied gradient descent algorithm to learn overcomplete dictionaries along each mode of the tensor (see [20] for definition of tensor modes). Peng *et al.* [15] presented a tensor dictionary learning algorithm based on Tucker model with Group-block-sparsity constraint on the core tensor with good performance.

In this paper, we present a novel multidimensional dictionary learning approach based on a notion of tensor-SVD proposed in [3, 12, 13]. Essentially the t-SVD is based on an operator theoretic interpretation of the 3rd order tensors [3], as linear operators over the set of 2-D matrices. This framework has recently been used for dictionary learning for 2-D images in [19], but the authors there employ a different algorithm and the problem considered is tomographic image reconstruction. Moreover we will also consider the problem of filling in missing data by sparse coding using the learned dictionary.

The paper is organized as follows. In section 2 we go over the definitions and notations, then illustrate the main differences and advantages over other tensor decomposition methods. Section 3 formulates the objective function for tensor dictionary learning problem using t-SVD, by introducing the “tubal sparsity” of third-order tensors. Our tensor dictionary learning model and detailed algorithm to

solve the problem are presented in Section 4. In Section 5 we show experiment results on third order tensor completion and denoising. Finally we conclude our paper in Section 6.

2. Brief Overview of T-SVD Framework

2.1. Notations and Preliminaries

In this part we briefly describe the notations used throughout the paper, and the t-SVD structure proposed in [3, 12, 13].

A tensor is a multidimensional array of numbers. For example, vectors are first order tensors, matrices are second order tensors. Tensors of size $n_1 \times n_2 \times n_3$ are called third order tensors. In this paper, third order tensors are represented in bold script font \mathcal{A} .

A *Slice* of an n -th order tensor is a 2-D section defined by fixing all but two indices. For a third order tensor \mathcal{A} , we will use the Matlab notation $\mathcal{A}(k, :, :)$, $\mathcal{A}(:, k, :)$ and $\mathcal{A}(:, :, k)$ to denote the k -th horizontal, lateral and frontal slices. $\mathcal{A}^{(k)}$ is particularly used to represent $\mathcal{A}(:, :, k)$, and $\vec{\mathcal{A}}_k$ represents $\mathcal{A}(:, k, :)$. We also call such $\vec{\mathcal{A}}_k$ *tensor columns*.

A *Fiber* (or *Tube*) is a 1-D section obtained by fixing all indices but one. For a third order tensor, $\mathcal{A}(:, i, j)$, $\mathcal{A}(i, :, j)$ and $\mathcal{A}(i, j, :)$ denote the (i, j) -th mode-1, mode-2 and mode-3 fiber. Specifically we let $\vec{a} \in \mathbb{R}^{1 \times 1 \times n_3}$ denote an n_3 -tube.

The approach in [3, 12, 13] rests on defining a multiplication operation, referred to as the tensor-product (t-product) between two third order tensors. This is done by using a commutative operation, in particular circular convolution between tensor tubes as defined below.

Definition 2.1.1. (t-product) The t-product between $\mathcal{A} \in \mathbb{R}^{n_1 \times n_2 \times n_3}$ and $\mathcal{B} \in \mathbb{R}^{n_2 \times n_4 \times n_3}$ is an $n_1 \times n_4 \times n_3$ tensor \mathcal{C} whose (i, j) -th tube $\mathcal{C}(i, j, :)$ is given by

$$\mathcal{C}(i, j, :) = \sum_{k=1}^{n_2} \mathcal{A}(i, k, :) * \mathcal{B}(k, j, :) \quad (1)$$

where $i = 1, 2, \dots, n_1$, $j = 1, 2, \dots, n_4$. When a third order tensor is viewed as a matrix of tubes along the third dimension, the t-product is analogous to the matrix multiplication except that the multiplication between numbers are replaced by the circular convolution between tubes.

Remark 2.1.1. From the relationship between circular convolution and Discrete Fourier Transform(DFT), the t-product of \mathcal{A} and \mathcal{B} can be computed efficiently in Fourier domain. Specifically, let $\hat{\mathcal{A}} = \text{fft}(\mathcal{A}, [], 3)$ and $\hat{\mathcal{B}} = \text{fft}(\mathcal{B}, [], 3)$ be the tensors obtained by taking the Fast Fourier Transform (FFT) along the tube fibers in third dimension of \mathcal{A} and \mathcal{B} , then we can compute the t-product of

\mathcal{A} and \mathcal{B} through the following,

$$\begin{aligned} \hat{\mathcal{C}}(:, :, i) &= \hat{\mathcal{A}}(:, :, i) * \hat{\mathcal{B}}(:, :, i), i = 1, 2, \dots, n_3 \\ \mathcal{C} &= \text{ifft}(\hat{\mathcal{C}}, [], 3) \end{aligned}$$

Definition 2.1.2. (Tensor transpose) The conjugate transpose of a tensor $\mathcal{A} \in \mathbb{R}^{n_1 \times n_2 \times n_3}$ is an $n_2 \times n_1 \times n_3$ tensor \mathcal{A}^T obtained by taking the conjugate transpose of each frontal slice of \mathcal{A} , then reversing the order of transposed frontal slices 2 through n_3 .

Definition 2.1.3. (Identity tensor) The identity tensor $\mathcal{J} \in \mathbb{R}^{n \times n \times n_3}$ is defined as follows,

$$\mathcal{J}(:, :, 1) = I_{n \times n}, \quad \mathcal{J}(:, :, k) = 0, k = 2, 3, \dots, n \quad (2)$$

where $I_{n \times n}$ is the identity matrix of size $n \times n$.

Definition 2.1.4. (Orthogonal Tensor) A tensor $\mathcal{Q} \in \mathbb{R}^{n \times n \times n_3}$ is orthogonal if it satisfies

$$\mathcal{Q}^T * \mathcal{Q} = \mathcal{Q} * \mathcal{Q}^T = \mathcal{J} \quad (3)$$

Definition 2.1.5. (f-diagonal Tensor) A tensor is called f-diagonal if each frontal slice of this tensor is a diagonal matrix.

2.2. Tensor Singular Value Decomposition(t-SVD)

We now define the tensor Singular Value Decomposition using the t-product introduced in previous section.

Definition 2.2.1. The t-SVD of a third-order tensor $\mathcal{M} \in \mathbb{R}^{n_1 \times n_2 \times n_3}$ is given by

$$\mathcal{M} = \mathcal{U} * \mathcal{S} * \mathcal{V}^T \quad (4)$$

where $*$ denotes the t-product, $\mathcal{U} \in \mathbb{R}^{n_1 \times n_1 \times n_3}$ and $\mathcal{V} \in \mathbb{R}^{n_2 \times n_2 \times n_3}$ are orthogonal tensors. $\mathcal{S} \in \mathbb{R}^{n_1 \times n_2 \times n_3}$ is a rectangular f-diagonal tensor.

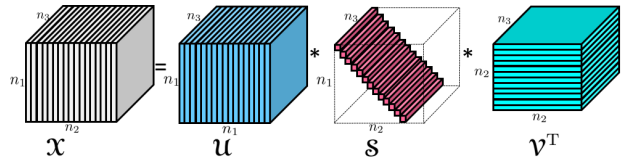


Figure 1: t-SVD of an $n_1 \times n_2 \times n_3$ tensor.

Figure 1 illustrates the t-SVD of 3rd order tensors. Similar to the t-product, we can also compute t-SVD in Fourier domain, see Algorithm 1.

As discussed in [23], t-SVD has many advantages over the classical tensor decompositions such as CANDECOP/PARAFAC [10] and Tucker [20]. For example, given a fixed rank, the computation of CANDECOP/PARAFAC decomposition can be numerically unstable, since calculating the rank-1 components in this

Algorithm 1 T-SVD of third order tensors

Input: $\mathcal{M} \in \mathbb{R}^{n_1 \times n_2 \times n_3}$
Output: $\mathbf{U} \in \mathbb{R}^{n_1 \times n_1 \times n_3}$, $\mathbf{V} \in \mathbb{R}^{n_2 \times n_2 \times n_3}$ and $\mathbf{S} \in \mathbb{R}^{n_1 \times n_2 \times n_3}$ such that $\mathcal{M} = \mathbf{U} * \mathbf{S} * \mathbf{V}^T$.
 $\widehat{\mathcal{M}} = \text{fft}(\mathcal{M}, [], 3)$;
for $i = 1$ **to** n_3 **do**
 $[\mathbf{U}, \mathbf{S}, \mathbf{V}] = \text{SVD}(\widehat{\mathcal{M}}(:, :, i))$
 $\widehat{\mathbf{U}}(:, :, i) = \mathbf{U}$; $\widehat{\mathbf{S}}(:, :, i) = \mathbf{S}$; $\widehat{\mathbf{V}}(:, :, i) = \mathbf{V}$;
end for
 $\mathbf{U} = \text{ifft}(\widehat{\mathbf{U}}, [], 3)$, $\mathbf{S} = \text{ifft}(\widehat{\mathbf{S}}, [], 3)$, $\mathbf{V} = \text{ifft}(\widehat{\mathbf{V}}, [], 3)$.

model is difficult. Similarly, finding the best Tucker multi-rank \vec{r} approximation to a tensor is numerically expensive and often does not yield the best fit to the original tensor. However, the computation of t-SVD is very easy since one only needs to do several SVDs as shown in Algorithm 1. Another very important property is the optimality approximation of t-SVD [13], described in the following.

Theorem 2.2.1. *Let $\mathcal{M} = \mathbf{U} * \mathbf{S} * \mathbf{V}^T$ be the t-SVD of $\mathcal{M} \in \mathbb{R}^{n_1 \times n_2 \times n_3}$. Then for $k < \min(n_1, n_2)$, define $\mathcal{M}_k = \sum_{i=1}^k \mathbf{U}(:, i, :) * \mathbf{S}(i, i, :) * \mathbf{V}(:, i, :)^T$, we have*

$$\mathcal{M}_k = \arg \min_{\tilde{\mathcal{M}} \in \mathbb{M}} \|\mathcal{M} - \tilde{\mathcal{M}}\|_F$$

where $\mathbb{M} = \{\mathcal{X} * \mathcal{Y} | \mathcal{X} \in \mathbb{R}^{n_1 \times k \times n_3}, \mathcal{Y} \in \mathbb{R}^{k \times n_2 \times n_3}\}$.

If we define *tensor tubal rank* of \mathcal{M} to be the number of non-zero diagonal tubes in \mathbf{S} [23], then this theorem is saying that \mathcal{M}_k is the closest tensor to \mathcal{M} in Frobenius norm among all tensors of tensor tubal rank at most k .

2.3. t-linear Combination of Tensor Dictionaries and Coefficients

As in the matrix case, given an overcomplete dictionary $D \in \mathbb{R}^{n \times K}$ which contains K prototype signal-atoms for columns, a signal $y \in \mathbb{R}^n$ can be represented as a linear combination of columns of D

$$y = Dx \quad (5)$$

where $x \in \mathbb{R}^K$ is called the representation coefficient vector of y . This set up could be easily extended to 3rd order tensors using the framework outlined in the previous section. Given K tensor columns (or dictionary atoms) $\vec{\mathcal{D}}_k \in \mathbb{R}^{n_1 \times 1 \times n_3}$, we represent a tensor signal $\vec{\mathcal{X}} \in \mathbb{R}^{n_1 \times 1 \times n_3}$ using the *t-linear combination* of the given tensor dictionaries as follows,

$$\vec{\mathcal{X}} = \sum_{k=1}^K \vec{\mathcal{D}}_k * \vec{c}_k = \mathcal{D} * \vec{\mathcal{C}} \quad (6)$$

where $\{\vec{c}_k\}_{k=1}^K$ are tubes of size $1 \times 1 \times n_3$; $\vec{\mathcal{C}} \in \mathbb{R}^{K \times 1 \times n_3}$ is called coefficient tensor obtained by aligning all the \vec{c}_k . $\mathcal{D} = \{\vec{\mathcal{D}}_1, \vec{\mathcal{D}}_2, \dots, \vec{\mathcal{D}}_K\} \in \mathbb{R}^{n_1 \times K \times n_3}$ is the tensor dictionary. The representation (6) may either be exact or approximate satisfying

$$\|\vec{\mathcal{X}} - \mathcal{D} * \vec{\mathcal{C}}\| \leq \epsilon \quad (7)$$

for some $\epsilon > 0$. When $K > n$, we say the tensor dictionary \mathcal{D} is overcomplete.

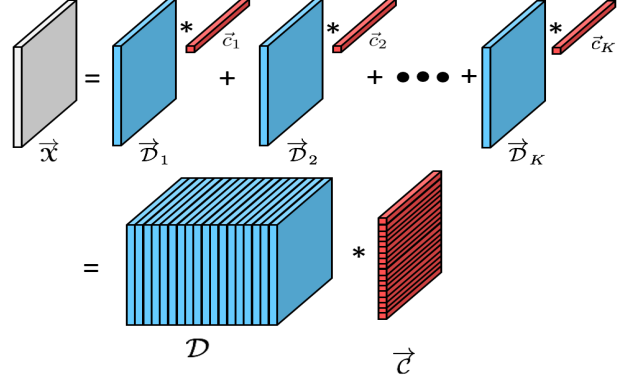


Figure 2: A tensor signal represented by a t-linear combination of K tensor dictionary atoms.

3. Problem Formulation

In this section, we introduce our tensor dictionary learning model and the related algorithm.

3.1. From Matrix to Tensor Dictionary Learning

Given an overcomplete dictionary $D \in \mathbb{R}^{n \times K}$ with $K > n$, if D is full rank, there are infinite number of solutions to the representation problem (5); therefore in order to constrain the solution set, one common approach is to enforce sparsity. As in classic dictionary learning model which was first designed for the purpose of reconstruction, one adaptively learns an overcomplete dictionary using the training data, which leads to the best possible representation of the data with sparsity constraints. Specifically, given training data $\{y_i\}_{i=1}^n \in \mathbb{R}^d$ where d is the dimensionality and n is the total number of training data used, dictionary learning methods aim at finding an overcomplete dictionary $D \in \mathbb{R}^{d \times K}$ with $K > d$, and a coefficient matrix $X = [x_1, x_2, \dots, x_n] \in \mathbb{R}^{K \times n}$ by the following optimization problem,

$$\begin{aligned} \min_{D, X} \quad & \sum_{i=1}^n \|y_i - Dx_i\|_F^2 \\ \text{subject to} \quad & \|x_i\|_q \leq T, \quad i = 1, 2, \dots, n \end{aligned} \quad (8)$$

where $\|\cdot\|_q, q \geq 1$ is the ℓ_q norm which represents different sparsity regularization.

Using t-SVD structure discussed in the previous section, we generalize this dictionary learning model to higher dimensional cases. Given training data as tensor columns $\{\vec{\mathbf{y}}_i\}_{i=1}^n \in \mathbb{R}^{d \times 1 \times n_3}$, we want to find a dictionary $\mathcal{D} \in \mathbb{R}^{n \times K \times n_3}$ with $K > n$, and “*tubal sparse*” tensor coefficients $\{\vec{\mathbf{x}}_i\}_{i=1}^n \in \mathbb{R}^{K \times 1 \times n_3}$ to represent the training data using t-product. The tubal sparsity of a tensor column is defined in [23] as follows.

Definition 3.1.1. (tensor tubal sparsity) Given a tensor column $\vec{\mathbf{x}}$, the tensor tubal sparsity $\|\cdot\|_{\text{TS}}$ is defined as the number of non-zero tubes of $\vec{\mathbf{x}}$ in the third dimension.

Then we can construct our dictionary learning model:

$$\begin{aligned} \min_{\mathcal{D}, \vec{\mathbf{x}}_i} \quad & \sum_{i=1}^n \|\vec{\mathbf{y}}_i - \mathcal{D} * \vec{\mathbf{x}}_i\|_F^2 \\ \text{subject to} \quad & \|\vec{\mathbf{x}}_i\|_{\text{TS}} \leq T, \quad i = 1, 2, \dots, n \end{aligned} \quad (9)$$

or equivalently,

$$\begin{aligned} \min_{\mathcal{D}, \mathbf{X}} \quad & \|\mathbf{Y} - \mathcal{D} * \mathbf{X}\|_F^2 \\ \text{subject to} \quad & \|\mathbf{X}\|_{\text{TS}} \leq T_0 \end{aligned} \quad (10)$$

where $\mathbf{Y} = [\vec{\mathbf{y}}_1, \vec{\mathbf{y}}_2, \dots, \vec{\mathbf{y}}_n] \in \mathbb{R}^{d \times n \times n_3}$ and $\mathbf{X} = [\vec{\mathbf{x}}_1, \vec{\mathbf{x}}_2, \dots, \vec{\mathbf{x}}_n] \in \mathbb{R}^{K \times n \times n_3}$. Figure 3 illustrates the tensor sparse coding model. Note that if the j th tube of $\vec{\mathbf{x}}_i(j, 1, :)$ is zero, then it means that the j th dictionary $\mathcal{D}(:, j, :)$ is not being used in the representation of $\vec{\mathbf{y}}_i$.

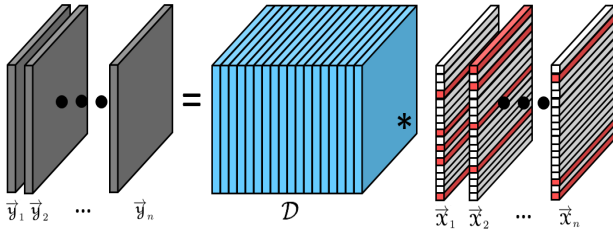


Figure 3: Data in the form of tensor columns represented by the t-product of tensor dictionary and tubal-sparse coefficient tensors. The red tubes in the coefficient tensors stand for the non-zero tubes and white ones are zero tubes.

3.2. K-TSVD

We now discuss our tensor dictionary learning model in details. Our model is called K-TSVD since it is a general extension from classic K-SVD to high dimensional tensor based on t-SVD. Similarly to K-SVD algorithm, K-TSVD

also consists of two stages: the tensor sparse coding stage and the tensor dictionary update stage. First let’s consider the sparse coding stage where the tensor dictionary \mathcal{D} is fixed. So we need to solve

$$\begin{aligned} \min_{\mathbf{X}} \quad & \|\mathbf{Y} - \mathcal{D} * \mathbf{X}\|_F^2 \\ \text{subject to} \quad & \|\mathbf{X}\|_{\text{TS}} \leq T_0 \end{aligned} \quad (11)$$

or alternatively we can work on an equivalent form,

$$\min_{\vec{\mathbf{x}}_i} \|\mathbf{Y} - \mathcal{D} * \mathbf{X}\|_F^2 + \lambda \|\mathbf{X}\|_{\text{TS}} \quad (12)$$

for some positive λ . Since the sparsity measure is computational intractable in both matrix and tensor cases, we use the $\|\cdot\|_{1,1,2}$ norm [23] instead as a convex relaxation for the tubal sparsity, where the $\|\cdot\|_{1,1,2}$ norm of a 3rd order tensor \mathbf{X} is defined as

$$\|\mathbf{X}\|_{1,1,2} = \sum_{i,j} \|\mathbf{x}(i, j, :)\|_F$$

If we regard a third dimensional tube $\vec{x} \in \mathbb{R}^{1 \times 1 \times n_3}$ as a $n_3 \times 1$ column vector, then the $\ell_{1,1,2}$ norm of \mathbf{X} is just the summation of ℓ_2 norm of all such tubes along the third dimension in \mathbf{X} .

Replacing the tubal sparsity with the $\ell_{1,1,2}$ norm, the problem becomes

$$\min_{\mathbf{X}} \|\mathbf{Y} - \mathcal{D} * \mathbf{X}\|_F^2 + \lambda \|\mathbf{X}\|_{1,1,2} \quad (13)$$

In order to solve this problem, one more definition is needed here. For a third order tensor $\mathcal{A} \in \mathbb{R}^{n_1 \times n_2 \times n_3}$, define the block diagonal form $\bar{\mathcal{A}}$ in Fourier domain as follows,

$$\bar{\mathcal{A}} = \text{blkdiag}(\hat{\mathcal{A}}) = \begin{bmatrix} \hat{\mathcal{A}}^{(1)} & & & \\ & \hat{\mathcal{A}}^{(2)} & & \\ & & \ddots & \\ & & & \hat{\mathcal{A}}^{(n_3)} \end{bmatrix} \quad (14)$$

where $\hat{\mathcal{A}} = \text{fft}(\mathcal{A}, [\], 3)$ and $\mathcal{A}^{(i)}$ is the i th frontal slice of \mathcal{A} . Then (13) can be equivalently reformulated in Fourier domain as

$$\min_{\hat{\mathbf{X}}} \|\bar{\mathbf{Y}} - \bar{\mathcal{D}} \hat{\mathbf{X}}\|_F^2 + \lambda \sqrt{n_3} \|\hat{\mathbf{X}}\|_{1,1,2}$$

where the $\sqrt{n_3}$ factor comes from the fact that $\|\mathbf{X}\|_F = \|\hat{\mathbf{X}}\|_F / \sqrt{n_3}$ [23]. Use the general framework of Alternating Direction Method of Multipliers (ADMM) [2], we can solve this optimization problem recursively with the follow-

ing algorithm:

$$\bar{\mathbf{X}}_{k+1} = \arg \min_{\bar{\mathbf{X}}} \|\bar{\mathbf{Y}} - \bar{\mathbf{D}}\bar{\mathbf{X}}\|_F^2 + \text{tr}(\bar{\mathbf{Q}}_k^T \bar{\mathbf{X}}) + \frac{\rho}{2} \|\bar{\mathbf{X}} - \bar{\mathbf{z}}_k\|_F^2 \quad (15)$$

$$\bar{\mathbf{z}}_{k+1} = \arg \min_{\bar{\mathbf{z}}} \|\bar{\mathbf{z}}\|_{1,1,2} + \frac{\rho}{2\lambda} \|\bar{\mathbf{X}}_{k+1} + \frac{1}{\rho} \bar{\mathbf{Q}}_k - \bar{\mathbf{z}}\|_F^2 \quad (16)$$

$$\bar{\mathbf{Q}}_{k+1} = \bar{\mathbf{Q}}_k + \rho(\bar{\mathbf{X}}_{k+1} - \bar{\mathbf{z}}_{k+1}) \quad (17)$$

where $\rho > 0$. (15) is essentially a least square minimization problem and we can separately solve it in each frontal slice of $\bar{\mathbf{X}}$ (or equivalently, each diagonal block of $\bar{\mathbf{X}}$). Let $\bar{\mathbf{C}}_{k+1} = \bar{\mathbf{X}}_{k+1} + \bar{\mathbf{Q}}_k/\rho$, the update of (16) is given by

$$\bar{\mathbf{z}}_{k+1}(i, j, :) = \left(1 - \frac{\lambda}{\rho \|\bar{\mathbf{C}}_k(i, j, :)\|_F}\right)_+ \bar{\mathbf{C}}_k(i, j, :) \quad (18)$$

$$\forall i = 1, 2, \dots, K, j = 1, 2, \dots, n$$

where $(\cdot)_+ = \max(0, \cdot)$.

The second stage of our tensor dictionary learning model is dictionary update. Given fixed $\bar{\mathbf{D}}$ and $\bar{\mathbf{X}}$, suppose we only want to update the k -th element of $\bar{\mathbf{D}}$, we can decompose the error term as follows,

$$\begin{aligned} & \|\bar{\mathbf{Y}} - \bar{\mathbf{D}} * \bar{\mathbf{X}}\|_F^2 \\ &= \left\| \bar{\mathbf{y}} - \sum_{j=1}^K \bar{\mathbf{D}}_j * \bar{\mathbf{X}}(j, :, :) \right\|_F^2 \\ &= \left\| \left(\bar{\mathbf{y}} - \sum_{j \neq k} \bar{\mathbf{D}}_j * \bar{\mathbf{X}}(j, :, :) \right) - \bar{\mathbf{D}}_k * \bar{\mathbf{X}}(k, :, :) \right\|_F^2 \\ &= \|\bar{\mathbf{E}}_k - \bar{\mathbf{D}}_k * \bar{\mathbf{X}}(k, :, :)\|_F^2 \\ &= \|\bar{\mathbf{E}}_k - \bar{\mathbf{D}}(:, k, :) * \bar{\mathbf{X}}(k, :, :)\|_F^2 \end{aligned}$$

$\bar{\mathbf{E}}_k$ here stands for the representation error when the k -th atom $\bar{\mathbf{D}}(:, k, :)$ is removed from the dictionary. The next step is to find $\bar{\mathbf{D}}(:, k, :) * \bar{\mathbf{X}}(k, :, :)$ which best approximates $\bar{\mathbf{E}}_k$, so that the error term is minimized. This is essentially to compute the best tubal rank-1 approximation using Theorem 2.2.1. Since we need to maintain the tubal sparsity of $\bar{\mathbf{X}}$ and don't want to fully fill $\bar{\mathbf{X}}(k, :, :)$, let $w_k = \{i | \bar{\mathbf{X}}(k, i, :) \neq 0, i = 1, 2, \dots, n\}$ be the set of indices where data $\bar{\mathbf{Y}}$ uses tensor dictionary $\bar{\mathbf{D}}(:, k, :)$ and restrict $\bar{\mathbf{E}}_k$ by choosing the tensor columns corresponding to w_k to obtain $\bar{\mathbf{R}}_k : \bar{\mathbf{R}}(:, i, :) = \bar{\mathbf{E}}(:, w_k(i), :), i = 1, 2, \dots, |w_k|$. From Theorem 2.2.1, we apply t-SVD on $\bar{\mathbf{R}}_k$ to get $\bar{\mathbf{U}}, \bar{\mathbf{S}}$ and $\bar{\mathbf{V}}$, and take the first tensor column of $\bar{\mathbf{U}}$ to update $\bar{\mathbf{D}}(:, k, :)$, use $\bar{\mathbf{S}}(1, 1, :) * \bar{\mathbf{V}}(:, 1, :)^T$ to renovate the coefficient tensors which use the k -th dictionary. To accelerate the algorithm we only compute the approximate rank-1

SVDs in Fourier domain when we compute t-SVD of $\bar{\mathbf{R}}$. The complete algorithm is presented in Algorithm 2.

Algorithm 2 K-TSVD

Input : Observed tensor data $\bar{\mathbf{Y}} = \{\bar{\mathbf{y}}_i\}_{i=1}^{n_2} \in \mathbb{R}^{n_1 \times n_2 \times n_3}$, $\lambda > 0$.

Initialize: Dictionary $\bar{\mathbf{D}}_0 \in \mathbb{R}^{n_1 \times K \times n_3}$

Repeat until convergence:

- 1: Compute the sparse coefficient tensor using (15)-(17):

$$\bar{\mathbf{X}} = \arg \min_{\bar{\mathbf{X}}} \|\bar{\mathbf{Y}} - \bar{\mathbf{D}} * \bar{\mathbf{X}}\|_F^2 + \lambda \|\bar{\mathbf{X}}\|_{1,1,2}$$

- 2: **for** $k = 1, 2, \dots, K$ **do**
- 3: Let $w_k = \{i | \bar{\mathbf{X}}(k, i, :) \neq 0\}$ be the set of indices where data $\bar{\mathbf{Y}}$ uses dictionary $\bar{\mathbf{D}}(:, k, :)$.
- 4: Compute $\bar{\mathbf{E}}_k = \bar{\mathbf{Y}} - \sum_{j \neq k} \bar{\mathbf{D}}(:, j, :) * \bar{\mathbf{X}}(j, :, :)^T$, which is the over all error without using the k -th dictionary atom $\bar{\mathbf{D}}(:, k, :)$.
- 5: Restrict $\bar{\mathbf{E}}_k$ by choosing only the tensor columns corresponding to w_k and obtain $\bar{\mathbf{R}}_k$:

$$\bar{\mathbf{R}}(:, i, :) = \bar{\mathbf{E}}(:, w_k(i), :) \quad (19)$$

for $i = 1, 2, \dots, |w_k|$.

- 6: Compute the t-SVD of $\bar{\mathbf{R}}_k$:

$$\bar{\mathbf{R}}_k = \bar{\mathbf{U}} * \bar{\mathbf{S}} * \bar{\mathbf{V}}^T.$$

- 7: Update $\bar{\mathbf{D}}(:, k, :) = \bar{\mathbf{U}}(:, 1, :)$.
- 8: Update $\bar{\mathbf{X}}(k, w_k, :) = \bar{\mathbf{S}}(1, 1, :) * \bar{\mathbf{V}}(:, 1, :)^T$.
- 9: **end for**

Output: Trained tensor dictionary $\bar{\mathbf{D}}$.

4. Experiment Results

4.1. Filling Missing Pixels in Tensors

In this section we consider the application of filling missing pixels in third order tensors. Suppose that we are given a video with dead pixels, where the dead pixels mean pixel values are deleted or missing on some fixed positions of each frame. Specifically, let Ω indicate the set of indices of the remaining pixels and $\bar{\mathbf{M}}$ be the data tensor, then $\bar{\mathbf{M}}(i, j, :) = 0$ for all $(i, j) \notin \Omega$. Our goal is to recover such tensors with missing pixels. Suppose $\bar{\mathbf{D}}$ is the learned over-complete dictionary on the training data, define P_Ω as an orthogonal projector such that $P_\Omega(\bar{\mathbf{M}})(i, j, :) = \bar{\mathbf{M}}(i, j, :)$, if $(i, j) \in \Omega$ and 0 otherwise. Then for each patch $\bar{\mathbf{M}}_k$ in the test data, the reconstruction of this patch is $\bar{\mathbf{D}} * \bar{\mathbf{C}}_k$, where $\bar{\mathbf{C}}_k$ is the solution to

$$\min_{\bar{\mathbf{C}}_k} \|P_\Omega(\bar{\mathbf{M}}_k) - P_\Omega(\bar{\mathbf{D}} * \bar{\mathbf{C}}_k)\|_F^2 + \lambda \|\bar{\mathbf{C}}_k\|_{1,1,2} \quad (20)$$

which can be solved in the same manner as (13).

We utilized a basketball video here to apply K-TSVD algorithm and reconstruct \mathcal{M} from missing pixels. There are 40 frames in the video and the resolution of each frame is 144×256 . To learn the overcomplete dictionary using K-TSVD, we randomly took 9000 overlapping block patches of size $8 \times 8 \times 10$ from the first 30 frames, saved them as tensor columns of size $64 \times 1 \times 10$, and obtained our training data \mathcal{Y} of total size $64 \times 9000 \times 10$. All these patches were used to train a tensor dictionary with $K = 256$ atoms. The last 10 frames of the video were used for testing. We took the total 576 disjoint $8 \times 8 \times 10$ blocks in the last 10 frames, saved each block into a tensor column, and obtained our training data of size $64 \times 576 \times 10$.

We investigated the performance of K-TSVD by comparing it with K-SVD and DCT. In K-SVD, in order to have a fair comparison, for each test frame we also randomly trained 10000 block patches of size 8×8 in the first 30 frames. We visualize an example of the overcomplete DCT dictionary, the K-SVD learned dictionary and the K-TSVD learned dictionary in Figure 4. One frame with 50% and 70% missing pixels and its reconstructions are shown in Figure 5. As one can see the reconstruction based on K-TSVD learned dictionary has a better quality. Figure 6 shows the reconstruction error (RE) comparison of those three approaches, where the error is computed via $RE = \sqrt{\|\mathcal{X} - \mathcal{X}_{rec}\|_F^2 / N}$, N is the total number of pixels in the data. We can see that when the percentage of missing pixels is small, all three methods perform equally well. With more missing pixels, K-TSVD gives better performance over the other two methods.

4.2. Multispectral Image and Video Denoising

In order to further test the proposed method, we applied our algorithm on multispectral/hyperspectral images and video data denoising. In the first experiment the multispectral data was from the **Columbia datasets**¹, each dataset contains 31 real-world images of size 512×512 and is collected from 400nm to 700nm at 10nm steps. In our experiment we resized each image into size of 205×205 , and took images of the last 10 bands to accelerate the speed of training tensor dictionaries. Therefore the total size of the tensor data we used here is $205 \times 205 \times 10$. Further work is required to fully deploy the algorithm in large-scale high order tensor applications.

For the noise model we consider the fixed-location defects without knowing the noisy positions, which commonly exists in video and multispectral images. On image of each bandwidth, some fixed pixel locations are corrupted with very high noise and our task is to recover the image. Specifically in our experiment we picked a sparse number of pixel locations and added Gaussian noise on these

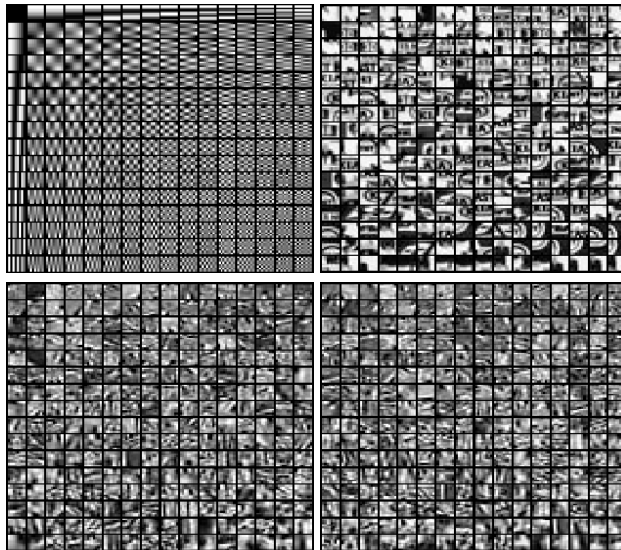


Figure 4: **Upper left:** The overcomplete DCT dictionary. **Upper right:** Dictionary learned on the first frame of the basketball video using K-SVD. **Lower left** The first frontal slice $\mathcal{D}(:, :, 1)$ of the learned dictionary of the tensor. **Lower right** The 3rd frontal slice $\mathcal{D}(:, :, 3)$ of the learned dictionary of the tensor.

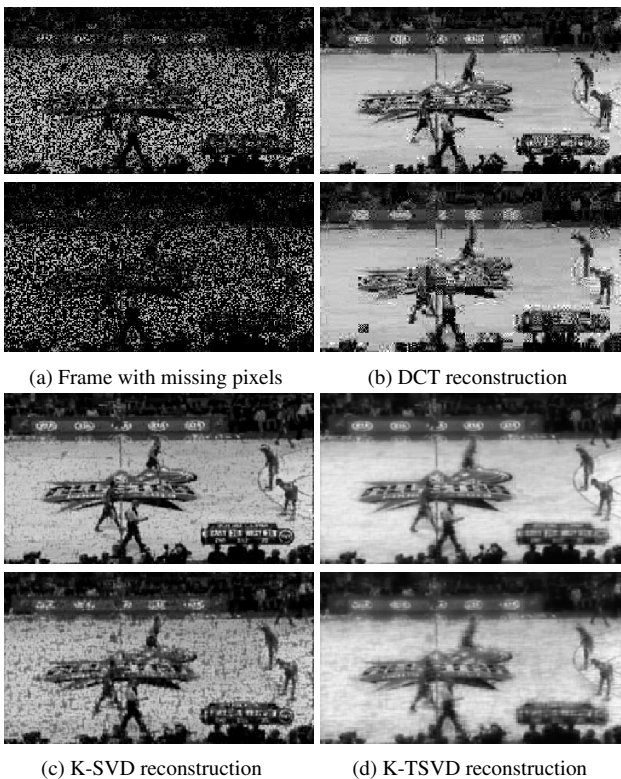


Figure 5: The reconstruction result from missing pixels on the basketball video. The different rows are for 50% and 70% of missing pixels respectively.

¹<http://www1.cs.columbia.edu/CAVE/databases/multispectral/>

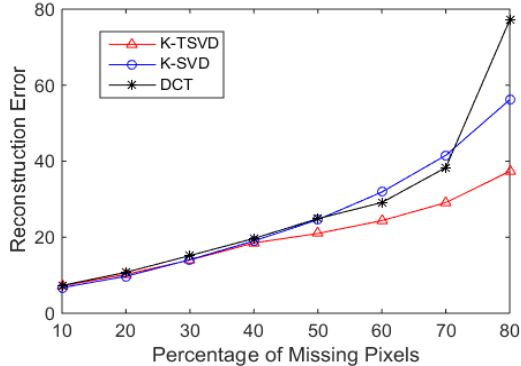


Figure 6: The reconstruction error comparison of DCT, K-SVD and K-TSVD on the reconstruction. The sparsity varies from 10% to 80%.

positions of each image. Let Ω indicate the set of noisy pixel locations, then what we did was for each $(i, j) \in \Omega$, $k = 1, 2, \dots, 10$, $\mathcal{Y}(i, j, k) = \mathcal{Y}(i, j, k) + w_{ijk}$, where \mathcal{Y} is the clean tensor and $w_{ijk} \sim \mathcal{N}(0, \sigma)$ is the additive Gaussian noise.

To train the data and learn the dictionaries, similarly to what we did in the previous experiment, we randomly took 10000 overlapping patches of size $8 \times 8 \times 10$ from the noisy tensor data, and saved each patch into a tensor column of size $64 \times 1 \times 10$. Therefore the tensor \mathcal{Y} to train here was of size $64 \times 10000 \times 10$. Since the total number of overlapping patches is $(205 - 7)^2 = 39204$, we only trained about a quarter of all the overlapping patches for the reason of computation time. If the size of data gets larger, then more patches are needed to ensure a more accurate dictionary. For a fair comparison, in K-SVD we also randomly select 10000 overlapping patches of size 8×8 within each noisy image. The trained dictionaries of KSVD and K-TSVD on the noisy tensor data are shown in Figure 7.

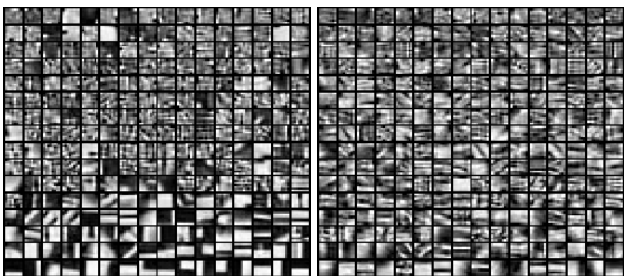


Figure 7: **Left** The learned dictionary on the first image using K-SVD. **Right** The first frontal slice $\mathcal{D}(:, :, 1)$ of the learned dictionary of the tensor.

The denoising process of our method includes a tensor sparse coding stage based on the learned tensor dictionary.

Table 1: PSNR(dB) of chart and stuffed toy images.

Sparsity	5%	10%	15%	10%	10%
Noise level	100	100	100	150	200
Noisy image	20.96	18.18	16.35	14.75	12.10
K-SVD	22.73	22.60	22.49	22.38	22.00
3DK-SVD	22.61	22.53	22.47	22.41	22.20
BM3D	26.95	26.62	26.36	25.23	24.29
LRTA	23.54	26.84	26.65	23.90	22.03
DNMDL	24.07	23.73	25.16	17.89	16.83
PARAFAC	27.07	26.86	26.72	26.13	25.24
KTSVD	27.19	26.98	26.79	26.18	25.44

We extracted each $8 \times 8 \times 10$ patch in the noisy multispectral images and solved the tensor sparse coding problem (13) to obtain the denoised patch. Following a similar idea in [6], we averaged all the denoised patches with some relaxation obtained by averaging with the original noisy data then got our denoised tensor.

To test the performance of our method, we compared our K-TSVD to these methods: K-SVD (band-wise) [1, 6] 3D K-SVD [6], BM3D (band-wise) [4], LRTA [17], DNMDL [15] and PARAFAC [14]. BM3D is a non-local denoising method based on an enhanced sparse representation in the transform domain, achieved by grouping similar patches into 3D data arrays. DNMDL is a Tucker dictionary learning based method, which like BM3D first groups the 3D patches and then use Tucker dictionary learning approach within each group to denoise. These two methods take the non-local similarity properties of different patches into consideration, and have very good denoising performance on some cases. LRTA is a Tucker3 based method which simply employs a low rank tensor approximation in Tucker3 model as denoised images. Similarly, PARAFAC is a CANDECOMP/PARAFAC based approach and it also obtains denoising result using a low CP rank approximation. Therefore these two methods can be regarded as a same type of denoising approach. K-SVD, 3DK-SVD and our method K-TSVD perform denoising by learning a over-complete dictionary on the noisy data and reconstruct the image using sparse coding, which is different from the other methods. The result with $\sigma = 100$ and the sparsity of noisy pixels equaling 10% is shown in Figure 8. The detailed PSNR comparison on different noise levels of these methods is in Table 1. We can see that our algorithm has a better performance over the other competing methods on most cases.

The second dataset we used was a set of hyperspectral images of natural scenes [8]. Similarly as before, we only took the images from bandwidth 630nm to 720nm and obtain a clean tensor of size $205 \times 268 \times 10$. We trained

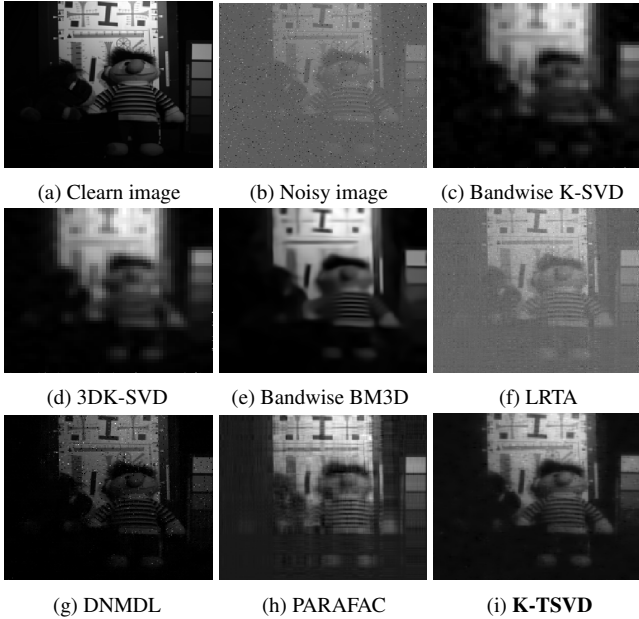


Figure 8: Denoised image at the 610nm band of chart and stuffed toy. The sparsity of the noisy pixels is 10% and the locations of noisy pixels are consistent on image of each band. The additive noise is Gaussian with $\sigma = 100$.

Table 2: PSNR(dB) of natural scene images.

Sparsity	5%	10%	15%	10%	10%
Noise level	100	100	100	150	200
Noisy image	21.29	18.02	16.45	14.62	12.19
K-SVD	22.81	22.70	22.64	22.51	22.28
3DK-SVD	22.78	22.73	22.71	22.66	22.58
BM3D	24.93	24.56	24.37	23.56	22.90
LRTA	25.64	25.68	26.12	23.76	21.96
DNMDL	22.01	23.40	24.62	20.68	18.47
PARAFAC	24.57	24.48	24.39	24.21	23.60
KTSVD	25.94	25.73	25.53	24.96	23.55

10000 dictionaries on the noisy data and perform denoising process using the same technique. The performance is shown in Figure 9 and the PSNR comparison on different noise levels is given in Table 2. In this dataset, the PSNR result shows that our algorithm also gives the good denoising performance on most cases. As one of the tensor based approach, LRTA gives the best PSNR on the case of sparsity 10% and standard deviation of the noise being 100. PARAFAC also works pretty well when sparsity equals 10% and noise level is 200.

We also applied K-TSVD algorithm on video denoising. The video that we used here was footage from a still camera

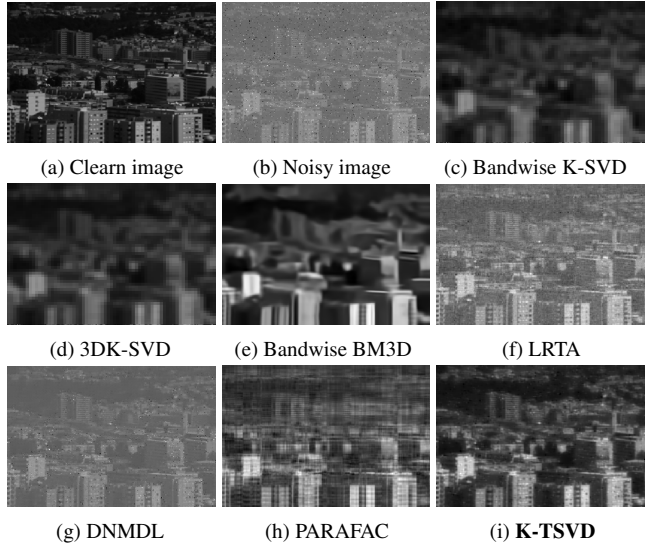


Figure 9: Denoised image at the 700nm band of hyperspectral images on natural scene. The sparsity of the noisy pixels is 10% and the locations of noisy pixels are consistent on image of each band. The additive noise is Gaussian with $\sigma = 100$.

view of a traffic intersection². The resolution of each frame is 175×328 , and we performed our method on every 10 frames. Figure 10 shows one frame of the denoising result with sparsity = 10% and noise level 100. As one can see in this experiment both LRTA and K-TSVD perform well.

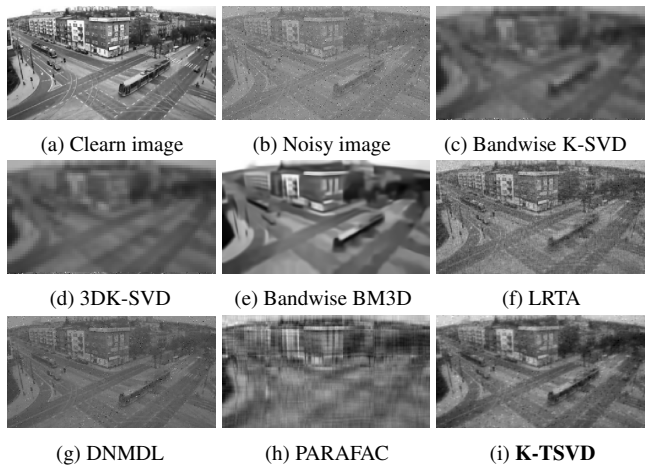


Figure 10: Video denoising result. The sparsity is 10% and $\sigma = 100$.

5. Conclusion

In this paper, we present a new method for tensor dictionary learning algorithm K-TSVD, using the t-SVD framework. Our main contribution lies in explicitly integrating

²www.changedetection.net

the sparse coding of third order tensors in t-SVD sense, and based on this we generalize the K-SVD dictionary learning model to deal with higher order tensors. The experimental results show that our approach yields very good performance on video completion and multispectral images denoising. Possible future work includes applying the group technique used in BM3D and DNMDL to process groups of similar patches separately.

References

- [1] M. Aharon, M. Elad, and A. Bruckstein. Svdd: An algorithm for designing overcomplete dictionaries for sparse representation. *Trans. Sig. Proc.*, 54(11):4311–4322, Nov. 2006. [1](#), [7](#)
- [2] S. Boyd, N. Parikh, E. Chu, B. Peleato, and J. Eckstein. Distributed optimization and statistical learning via the alternating direction method of multipliers. *Found. Trends Mach. Learn.*, 3(1):1–122, Jan. 2011. [4](#)
- [3] K. Braman. Third-order tensors as linear operators on a space of matrices. *Linear Algebra and its Applications*, pages 1241–1253, 2010. [1](#), [2](#)
- [4] K. Dabov, A. Foi, V. Katkovich, and K. Egiazarian. Image denoising by sparse 3d transform-domain collaborative filtering. *IEEE TRANS. IMAGE PROCESS*, 16(8):2080, 2007. [7](#)
- [5] G. Duan, H. Wang, Z. Liu, J. Deng, and Y. Chen. K-CPD: learning of overcomplete dictionaries for tensor sparse coding. In *Proceedings of the 21st International Conference on Pattern Recognition, ICPR 2012, Tsukuba, Japan, November 11-15, 2012*, pages 493–496, 2012. [1](#)
- [6] M. Elad and M. Aharon. Image denoising via sparse and redundant representations over learned dictionaries. *Trans. Img. Proc.*, 15(12):3736–3745, Dec. 2006. [7](#)
- [7] K. Engan, S. O. Aase, and J. H. Husøy. Multi-frame compression: theory and design. *Signal Processing*, 80(10):2121–2140, 2000. [1](#)
- [8] D. H. Foster, K. Amano, S. M. C. Nascimento, and M. J. Foster. Frequency of metamerism in natural scenes. *J. Opt. Soc. Am. A*, 23(10):2359–2372, Oct 2006. [7](#)
- [9] Y. Fu, J. Gao, Y. Sun, and X. Hong. Joint multiple dictionary learning for tensor sparse coding. In *2014 International Joint Conference on Neural Networks, IJCNN 2014, Beijing, China, July 6-11, 2014*, pages 2957–2964, 2014. [1](#)
- [10] R. A. Harshman. Foundations of the PARAFAC procedure: Models and conditions for an “explanatory” multimodal factor analysis. *UCLA Working Papers in Phonetics*, 16(1):84, 1970. [2](#)
- [11] F. Huang and A. Anandkumar. Convolutional dictionary learning through tensor factorization. *CoRR*, abs/1506.03509, 2015. [1](#)
- [12] M. Kilmer, K. Braman, and N. Hao. Third order tensors as operators on matrices: A theoretical and computational framework. *Tufts University, Department of Computer Science, Tech. Rep.*, January 2011. [1](#), [2](#)
- [13] M. E. Kilmer and C. D. Martin. Factorization strategies for third-order tensors. *Linear Algebra and its Applications*, 435(3):641 – 658, 2011. Special Issue: Dedication to Pete Stewart on the occasion of his 70th birthday. [1](#), [2](#), [3](#)
- [14] X. Liu, S. Bourennane, and C. Fossati. Denoising of hyperspectral images using the PARAFAC model and statistical performance analysis. *IEEE T. Geoscience and Remote Sensing*, 50(10):3717–3724, 2012. [7](#)
- [15] Y. Peng, D. Meng, Z. Xu, C. Gao, Y. Yang, and B. Zhang. Decomposable nonlocal tensor dictionary learning for multispectral image denoising. In *Proceedings of the 2014 IEEE Conference on Computer Vision and Pattern Recognition, CVPR ’14*, pages 2949–2956, Washington, DC, USA, 2014. IEEE Computer Society. [1](#), [7](#)
- [16] I. Ramirez, P. Sprechmann, and G. Sapiro. Classification and clustering via dictionary learning with structured incoherence and shared features. In *Computer Vision and Pattern Recognition (CVPR), 2010 IEEE Conference on*, pages 3501–3508, June 2010. [1](#)
- [17] N. Renard, S. Bourennane, and J. Blanc-Talon. Denoising and dimensionality reduction using multilinear tools for hyperspectral images. In *IEEE Trans. Geoscience and Remote Sensing*, 2008. [7](#)
- [18] R. Rubinstein, M. Zibulevsky, and M. Elad. Efficient implementation of the k-svd algorithm using batch orthogonal matching pursuit, 2008. [1](#)
- [19] S. Soltani, M. E. Kilmer, and P. C. Hansen. A tensor-based dictionary learning approach to tomographic image reconstruction. *CoRR*, abs/1506.04954, 2015. [1](#)
- [20] L. R. Tucker. Some mathematical notes on three-mode factor analysis. *Psychometrika*, 31:279–311, 1966c. [1](#), [2](#)
- [21] J. Yang, Z. Wang, Z. Lin, S. Cohen, and T. Huang. Coupled dictionary training for image super-resolution. *Image Processing, IEEE Transactions on*, 21(8):3467–3478, Aug 2012. [1](#)
- [22] Q. Zhang and B. Li. Discriminative k-svd for dictionary learning in face recognition. In *CVPR*, pages 2691–2698. IEEE Computer Society, 2010. [1](#)
- [23] Z. Zhang, G. Ely, S. Aeron, N. Hao, and M. E. Kilmer. Novel methods for multilinear data completion and de-noising based on tensor-svd. In *2014 IEEE Conference on Computer Vision and Pattern Recognition, CVPR 2014, Columbus, OH, USA, June 23-28, 2014*, pages 3842–3849, 2014. [2](#), [3](#), [4](#)
- [24] S. Zubair and W. Wang. Tensor dictionary learning with sparse tucker decomposition. In *Digital Signal Processing (DSP), 2013 18th International Conference on*, pages 1–6, July 2013. [1](#)